ELSEVIER

Earth and Planetary Science Letters 142 (1996) 59–74

EPSL

Neogene Himalayan weathering history and river $^{87}Sr/^{86}Sr$: impact on the marine Sr record

Louis A. Derry [a,b,*], Christian France-Lanord [b,1]

[a] *Cornell University, Department of Geological Sciences, Ithaca, NY 14853, USA*

[b] *Centre de Recherches Pétrographiques et Géochimiques — CNRS, B.P. 20, 54501 Vandoeuvre-les-Nancy, France*

Received 1 July 1995; accepted 26 April 1996

Abstract

Clastic sediments in the Bengal Fan contain a Neogene history of erosion and weathering of the Himalaya. We present data on clay mineralogy, major element, stable and radiogenic isotope abundances from Lower Miocene–Pleistocene sediments from ODP Leg 116. Nd and Sr isotope data show that the Himalayan provenance for the eroded material has varied little since > 17 Ma. However, from 7 to 1 Ma smectite replaces illite as the dominant clay, while sediment accumulation decreased, implying an interval of high chemical weathering intensity but lower physical erosion rates in the Ganges–Brahmaputra (GB) basin. O and H isotopes in clays are correlated with mineralogy and chemistry, and indicate that weathering took place in the paleo-Gangetic flood plain. The $^{87}Sr/^{86}Sr$ ratios of pedogenic clays (vermiculite, smectite) record the isotopic composition of Sr in the weathering environment, and can be used as a proxy for $^{87}Sr/^{86}Sr$ in the paleo-GB basin. The Sr data from pedogenic clays shows that river $^{87}Sr/^{86}Sr$ values were near 0.72 prior to 7 Ma, rose rapidly to ≥ 0.74 in the Pliocene, and returned to ≤ 0.72 in the middle Pleistocene. These are the first direct constraints available on the temporal variability of $^{87}Sr/^{86}Sr$ in a major river system. The high $^{87}Sr/^{86}Sr$ values resulted from intensified chemical weathering of radiogenic silicates and a shift in the carbonate–silicate weathering ratio. Modeling of the seawater Sr isotopic budget shows that the high river $^{87}Sr/^{86}Sr$ values require a ca. 50% decrease in the Sr flux from the GB system in the Pliocene. The relationship between weathering intensity, $^{87}Sr/^{86}Sr$ and Sr flux is similar to that observed in modern rivers, and implies that fluxes of other elements such as Ca, Na and Si were also reduced. Increased weathering intensity but reduced Sr flux appears to require a late Miocene–Pliocene decrease in Himalayan erosion rates, followed by a return to physically dominated and rapid erosion in the Pleistocene. In contrast to the view that increasing seawater $^{87}Sr/^{86}Sr$ results from increased erosion, Mio–Pliocene to mid-Pleistocene changes in the seawater Sr budget were the result of reduced erosion rates and Sr fluxes from the Himalaya.

Keywords: Himalayas; ODP Site 717; ODP Site 718; Sr-87/Sr-86; Neogene; clay mineralogy; weathering

1. Introduction

A driving function for geochemical cycling is uplift and erosion. In order to trace the behavior of the geochemical cycle through time, it is useful to have constraints on past variations in erosion rates.

* Corresponding author. E-mail: derry@geology.cornell.edu

[1] E-mail: cfl@crpg.cnrs-nancy.fr

PII S0012-821X(96)00091-X

While proxies for past chemical weathering fluxes exist, such as the isotopic composition of marine Sr, their interpretation is not straightforward. An estimate of past weathering fluxes is difficult to make using isotopic tracers in seawater, because each of the available systems has multiple sources, leading to necessarily non-unique interpretations. Recent interest has been focused on the potential role of chemical weathering in the Himalaya as a source for changes in the cycle of marine strontium (and by analogy other elements) [1–8]. The principal cause of uncertainty in interpreting the Cenozoic marine Sr record in terms of weathering fluxes has been lack of constraints on the variation in the isotopic composition of the weathering flux of Sr through time. Very little is currently known about how the $^{87}Sr/^{86}Sr$ of river fluxes to the oceans may have varied, but without this information the mass balance for Sr isotopes in seawater is under-constrained. Sr measurements in fresh water carbonates have been used to reconstruct past isotopic variations in a single drainage basin [9]. Attempts to address this situation globally have included assuming a simple history for riverine $^{87}Sr/^{86}Sr$ values [5], presenting a series of 'either or' scenarios [4], or combining the Sr record with another tracer sensitive to weathering, such as Nd isotopes [1,10]. The results of these and other investigations suggest that variations in the Sr flux from the Himalaya have played an important, but as yet poorly quantified, role in the Cenozoic increase of the marine $^{87}Sr/^{86}Sr$ ratio.

Clay (and other secondary) minerals comprise the physical evidence of past silicate weathering processes. The mineralogy, sedimentology, chemistry and isotopic compositions of weathering products from the Himalaya thus provide a record of ancient weathering environments and fluxes in that region. A record of the erosional history of the Himalaya exists in the Bengal Fan, fed by the Ganges and Brahmaputra rivers. ODP has obtained a record of sedimentation since the early Miocene in the distal portion of the Bengal Fan, which provides a unique view of Himalayan erosion. In this paper we address the issue of isotopic variability in the weathering flux of Sr from the Himalaya during the Neogene, given the potential importance of this source for the evolution marine Sr. We also present data that constrain how weathering environments and processes have varied in the Himalayan region over the last 20 Ma. This study builds on our earlier work that defined the provenance of sediments in the Bengal Fan using isotopic tracers [11].

2. Analytical methods

Sediment samples from ODP Leg 116, Holes 717C and 718C, were selected to provide a range in age and sedimentary facies. Samples were first disaggregated in distilled water. The samples were wet-sieved to remove the > 50 μm coarse fraction. Mono-mineralic separates were prepared from the coarse fraction by hand picking. The preparation of < 2 μm and 2–50 μm fractions is described in [11]. Briefly, the samples were dispersed by agitation with Amberlite cation exchange resin (Na form) and distilled water. The < 2 μm fraction was then separated by gravity settling. The suspended 2 μm clays were decanted, and in some cases centrifuged to separate the 0.1 μm fraction. Then 1 ml of a clean $MgCl_2$ solution (Prolabo Normapur®) was added to flocculate the clays. This sequence was repeated as necessary. The flocculated 2–50 μm, < 2 μm and < 0.1 μm fractions were then separated from solution by centrifugation. The quality of the grain size separations was periodically checked using a microscope-mounted image processing system. In all cases the size separation technique was found to be highly effective. Aliquots of the < 2 μm or < 0.1 μm fractions were analyzed by standard XRD techniques for clay mineral identification.

Carbonate and remaining surface-adsorbed cations were removed from clay fractions by leaching with 10% acetic acid in an ultrasonic bath. Samples for Sr and Nd isotopic analysis were roasted at 700°C in platinum crucibles to remove organic matter. Samples were then weighed and spiked, and dissolved in a $HF–HNO_3–HClO_4$ mixture. Chromatographic separation of Rb, Sr, Sm and Nd followed standard procedures. Blanks for size-fractionated samples are conservatively estimated at ca. ≤ 0.5 ng for Nd and ≤ 1 ng for Sr (blank $^{87}Sr/^{86}Sr \approx 0.710$). These high blanks result from the complex sample preparation procedure. However, samples sizes were sufficiently large that blank corrections are not necessary.

Oxygen from clays was extracted by fluorination

using BrF_5. Samples were loaded in nickel tubes under dry N_2 atmosphere after dehydration at 120°C. For hydrogen, water was released from clays by heating at ca. 1400°C in silica tubes after overnight degassing at 150°C. Water was converted to H_2 over uranium at 800°C. High organic matter contents in some clay samples precluded analysis for H and O. H_2 and CO_2 gas were analyzed on a VG 602D mass spectrometer. Reproducibility on clay samples is $\pm 0.4‰$ for O and $\pm 2‰$ for H.

3. History and sources of sediment

The Bengal Fan (Fig. 1) receives sediment from the Himalaya delivered by the Ganges and Brahmaputra rivers. The Fan was established in the late Eocene and appears to have prograded rapidly toward the south during the latest Oligocene–early Miocene [12,13]. A direct record of sedimentation in the Bengal Fan since > 17 Ma is available from ODP Leg 116 [14]. Variations in lithology, sedimentation rate, grain size and clay mineralogy define three main intervals of deposition (Figs. 2 and 6). Prior to 7.4 Ma and after 0.9 Ma sedimentation rates were high, and lithologies were predominantly monotonous silts with illite and chlorite-rich clay fractions (the IC assemblage). Between 7.4 Ma and 0.9 Ma, deposition rates were lower and mean grain size finer. Sediments are mostly muds with smectite and kaolinite clays (the SK assemblage), intercalated with occasional, coarser, illite-rich layers [11,15,16].

Nd and Sr isotopic data can trace the provenance of the sediments deposited in the Bengal Fan [11,17]. There are several potential sources for the large volume of Bengal Fan sediments — each of these has a distinctive set of isotopic characteristics. These include the High Himalayan Crystalline (HHC) of paragneisses and granites ($^{87}Sr/^{86}Sr \approx 0.75$, $\epsilon_{Nd} \approx -16$); the Lesser Himalaya (LH), including Proterozoic–Cambrian(?) sediments and metasediments ($^{87}Sr/^{86}Sr \geq 0.8$, $\epsilon_{Nd} \approx -25$); and the Tibetan Sedimentary Series (TSS), Tethyan marine sediments exposed in the High Himalaya and Tibet ($^{87}Sr/^{86}Sr \leq 0.72$, $\epsilon_{Nd} \approx -12$ to -4). ϵ_{Nd} values from Bengal Fan turbidites vary little with age/depth, remaining near -16 ± 2 since the early Miocene (Fig. 2). Similar ϵ_{Nd} values are found in different mineral separates and size fractions, as well as whole rock samples. Sr isotopic values from Bengal Fan turbidites are 0.74–0.76 for most samples, similar to HHC values [11]. Exceptions include biotite separates, which have experienced significant radiogenic in-growth of ^{87}Sr, and some clay mineral separates, discussed below. The isotopic data show that the primary source for the Bengal Fan turbidites since the early Miocene has been the HHC, or a close analogue. The contribution from the TSS and the LH does generally not exceeded 20%, despite significant changes in sedimentation rate, lithology, mineralogy and degree of chemical weathering of the sediments [11]. An explanation dependent on mixing of different sources, rather than the dominance of a single source, to yield sediments with a relatively narrow

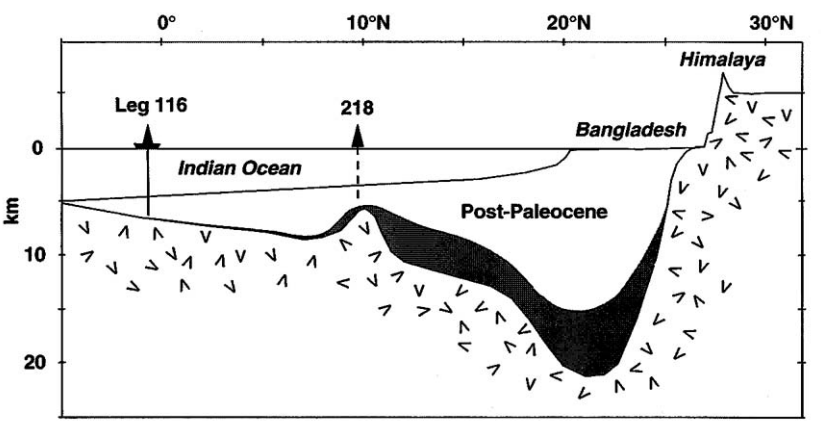

Fig. 1. Longitudinal cross section from Himalaya to southern Bengal basin showing location of Leg 116 sites and DSDP Hole 218, redrawn after [12].

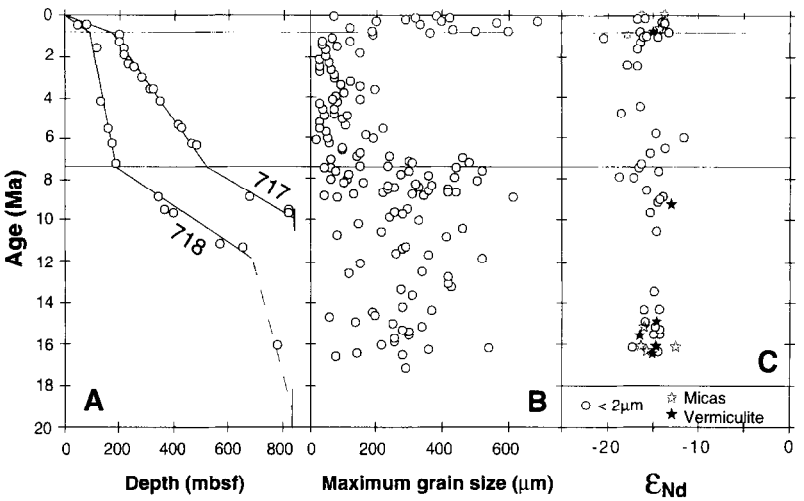

Fig. 2. (A) Sediment thickness [47], (B) maximum quartz grain size (MQGS) [14] and (C) ϵ_{Nd} of < 2 μm fractions, coarse vermiculites and micas (data from Table 1 and [17]) as a function of age in the distal Bengal Fan. Ages were recalculated according to [48]. The curves are for the ODP Leg 116 holes 717C and 718C. Low sedimentation rates are found between 7.4 Ma and 0.9 Ma, and are correlated with a decrease in MQGS and a lithologic shift from silts and sands to muds. Despite these sedimentological changes, ϵ_{Nd} values for different mineral and size fractions remain near -16 ± 2, indicating that the provenance of the turbidite sediments is dominated by the HHC at all intervals [11].

range of Sr and Nd compositions over the last 20 Ma is untenable. Widely different sample types, including mineral separates (feldspar, muscovite and biotite), grain-size fractions, and different clay assemblages, all have similar ϵ_{Nd} values [11]. Thus, the mixing process would have had to produce the same geochemical signature from hydrodynamically very different materials all the time since 20 Ma, despite changes in uplift, transport, climate and other boundary conditions.

Neodymium isotopic data from clay mineral separates (vermiculite and < 2 μm fractions) provide constraints on the sources of the different clay mineral assemblages in the Bengal Fan. ϵ_{Nd} data are plotted against K_2O/Al_2O_3 (an index of chemical alteration) for different size fractions in Fig. 3. Samples from the 50–2 μm fraction fall within the field defined by their HHC source rocks, and represent material that has undergone little chemical weathering. Clay samples (< 2 μm) from before 7.4 Ma or after 0.9 Ma are characterized by the IC clay assemblage. These samples have slightly higher ϵ_{Nd} values than whole rock or 50–2 μm fractions, although still within the field defined by the HHC. The difference in K_2O/Al_2O_3 between the two fractions is caused

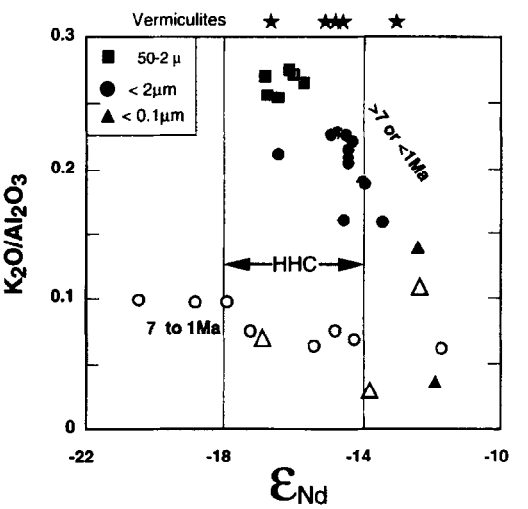

Fig. 3. Relationship between ϵ_{Nd} and K_2O/Al_2O_3 for different size fractions. K_2O/Al_2O_3 is an index of chemical weathering intensity. Open symbols = 7–1 Ma; filled symbols = > 7 or < 1 Ma; *HHC* = The High Himalaya Crystalline series of high-grade metamorphics and granites, the principal source of detrital material since the early Miocene, with ϵ_{Nd} typically -16 ± 2 [11]. The trend of increasing ϵ_{Nd} with decreasing grain size for < 2 μm IC samples from before 7.4 Ma or after 0.9 Ma reflects the contribution of a fine-grained, high ϵ_{Nd} component (10–20%), probably smectites derived from the weathering of volcanics. This component is insignificant for the mass balance of the whole rock.

by 10–25% of kaolinite ± smectite present in the < 2 μm IC fraction. Clays (< 2 μm) from 7.4 to 0.9 Ma contain the SK assemblage, and have ϵ_{Nd} values in the same range as other Bengal Fan samples, implying that the provenance of the SK assemblage is also primarily the HHC. K_2O/Al_2O_3 ratios are distinctly lower than for the IC samples, and are the result of more intense alteration during the production of smectites and kaolinite.

Four samples, of which three are from < 0.1 μm fractions, have ϵ_{Nd} values near -12. These samples suggest the presence of an additional source component associated with very fine-grained material that is high in ϵ_{Nd}. While we cannot uniquely identify this component, it is plausible that clays (smectites) derived from weathering of volcanic rocks, either in the Gangdese belt of Tibet or the Deccan province of India ($\epsilon_{Nd} \approx 0$), are the source of the extremely fine-grained, radiogenic component suggested by Fig. 3. The slightly higher ϵ_{Nd} values in the < 2 μm IC clays compared to the 50–2 μm fraction is probably the result of mixing with a component of this type. In any case, this component is volumetrically insignificant in the Fan as a whole.

4. Regional significance of Leg 116 observations

Given the enormous size of the Bengal Fan (Fig. 1), it is important to address the regional significance of sedimentological variations recorded at the Leg 116 sites. Several lines of evidence imply that the first order sedimentological changes observed at Leg 116 sites are derived from changes in the overall flux of sediment from the GB basin rather than from shifts in depocenters, either from onshore to offshore or within the fan itself:

(1) Similar patterns of sedimentation are seen at DSDP Site 218, which is located 1100 km northeast of the Leg 116 sites (Fig. 1). At Site 218 sedimentation rates decline and clay mineralogy shifts from illite-rich to smectite-rich assemblages in the late Miocene [18,19]. The occurrence of correlative lithologies, grain size distributions, sedimentation rate and clay mineral assemblages at three different Leg 116 sites, located near 1°S, and at Site 218, located at 8°N, demonstrates that the important variations in the sedimentation history are regional phenomena. Data from the Indus Fan (DSDP Site 222) also show a late Miocene decrease in sedimentation [20], suggesting that these late Miocene changes are general across the Himalayan front.

(2) The $\delta^{13}C$ values of total organic carbon at sites 717 and 718 are highly correlated with sedimentological changes since 7.4 Ma [8]. The $\delta^{13}C$ shift results from the expansion of C4 photosynthetic plants across the GB basin [21,22]. This correlation implies that processes in the foreland basin control both the sources of organic carbon and the composition and delivery of sediment to the fan.

(3) Pimm [23] noted that clastic sediment pulses could be correlated over long distances within the Bengal and Nicobar fans. Such a wide geographic dispersion precludes channel switching or other changes in the location of depocenters as an explanation for the long-term variations in sedimentation rate and lithology. It is also improbable that simply changing the channel network in the Fan, without a change in sediment source, could result in radical changes in the composition of the clay fraction.

(4) Finally, studies of other submarine fans suggest that levee construction takes place on a 10^5 year time scale, but the major variations in sediment composition observed at the Leg 116 sites and Site 218 are of 10^6 years duration, implying that simple construction of underwater structures is not the process responsible for the long-term sedimentological variations [24].

The implications of the basin-wide nature of stratigraphic events in the Bengal Fan are that the sedimentological variations are caused by: (1) changes in provenance; and/or (2) changes in transport phenomena in the Ganges watershed or near the head of the Bengal Fan complex.

5. Stable isotopic constraints on weathering processes

Due to the fact that the range of ϵ_{Nd} values in samples with the SK clay assemblage is nearly identical to the range found in other sediments of the Bengal Fan, we infer that the SK clays deposited from ca. 7.4 Ma to 0.9 were derived from chemical weathering of material similar to the less altered IC assemblage. XRD analyses of all < 2 μm clay

fractions show the presence of a mixture of illite, chlorite, smectite, kaolinite and mixed layer clays — the most abundant phases are either smectite or illite [15]. Clearly resolvable illite peaks are found even in < 0.1 μm fractions. Feldspar, and mica weathering to smectite and kaolinite results in a net loss of K, hence the K_2O/Al_2O_3 ratio varies with the extent of weathering and neoformation. Oxygen isotopic variations in the clays are correlated with both mineralogy and with K_2O/Al_2O_3 (Fig. 4). Illite-rich clays from the Bengal Fan are unusually low in ^{18}O compared to most low-temperature sedimentary illites, and are within a few per mil of values from HHC metamorphic rocks (Fig. 5). The low $\delta^{18}O$ and high K_2O/Al_2O_3 values in the IC samples imply that they are derived from high-temperature sources by physical erosion, with relatively little low-temperature alteration. Decreasing K_2O/Al_2O_3 in SK samples is accompanied by a shift toward higher $\delta^{18}O$ values, indicating formation at low temperature. We interpret the correlation of $\delta^{18}O$ with K_2O/Al_2O_3 in the clay fractions as a mixing relation between newly formed pedogenic material and a 'primary' end-member composed of illite derived from micas ($K_2O/Al_2O_3 \approx 0.33-0.45$) and chlorite ($K_2O/Al_2O_3 \approx 0$) with $\delta^{18}O$ given by values for micas from the HHC (8–10‰) [25]. Based on major element and mineralogical mass balance, the $\delta^{18}O$ value of the 'secondary' (smectite–kaolinite) end-member is estimated to lie between 26‰ and 28‰.

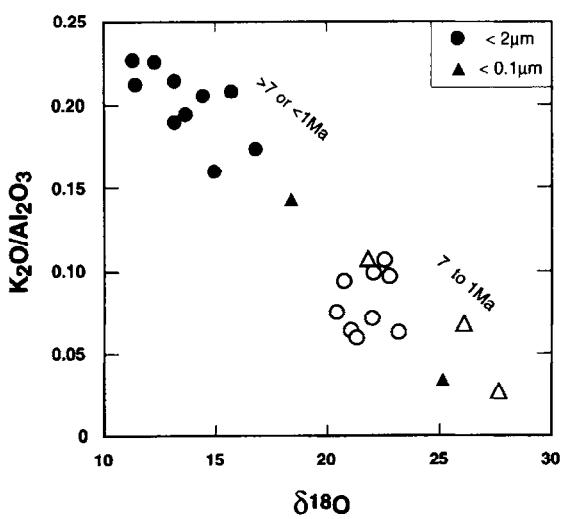

Fig. 4. $\delta^{18}O$ vs. K_2O/Al_2O_3 for clay fractions (< 2 μm and < 0.1 μm). Open symbols = 7–1 Ma; filled symbols = > 7 or < 1 Ma. Variations in clay composition can be interpreted as mixtures between illite + chlorite derived from metamorphic rocks primarily by physically erosion, which have near-metamorphic $\delta^{18}O$ values, and smectite ± kaolinite produced by chemical weathering, with $\delta^{18}O$ values indicating extensive low-temperature meteoric water interaction.

Due to the steep gradients in altitude and mean annual temperature in the Himalayan region, there are large variations in the stable isotopic composition of meteoric water ([26] and Fig. 5). Combined hydrogen and oxygen isotope data from clays can be used to locate the zone of intense weathering. In a $\delta^{18}O$ vs. δD diagram (Fig. 5) we compare Bengal Fan clays to calculated fields for smectite in equilibrium with modern surface water in the Himalaya and the GB plain at 20°C, and with seawater at 3°C. Modern Himalayan surface water is too depleted in D and ^{18}O to be the source for the Bengal Fan SK clay fractions. In contrast, meteoric water in the GB plain is compatible with the compositions of the SK clays.

The smectite end-member has $\delta^{18}O$ of 26–28‰, which is higher than calculated equilibrium values with modern water in the GB plain. There are several possible explanations for this difference:

(1) O-isotope exchange with seawater or pore water in the fan. This is unlikely, because: (i) δD values of secondary clays are significantly lower than expected for equilibrium with seawater or Bengal Fan pore water (≈ -5‰ [27]); and (ii) $^{87}Sr/^{86}Sr$ ratios of the smectite-rich samples are far from equilibrium with seawater (Table 1). It is improbable that the clays could have achieved oxygen isotope equilibrium with pore waters while remaining far from equilibrium with respect to D/H and Sr isotopes.

(2) Higher $\delta^{18}O$ values of paleometeoric water. The highest $\delta^{18}O$ smectites would require water as high as 0‰, which is only possible at these latitudes under desert conditions. The available constraints on past $\delta^{18}O$ values for surface water from soil carbonates do not indicate any period of higher values than at present but, rather, lower values prior to ca. 8 Ma [22]. This hypothesis is also inconsistent with the D/H data, which do not shift in the same sense.

(3) We suspect that the problem lies with the estimates of oxygen isotope fractionation in the smectite–water system. Oxygen isotope fractionation

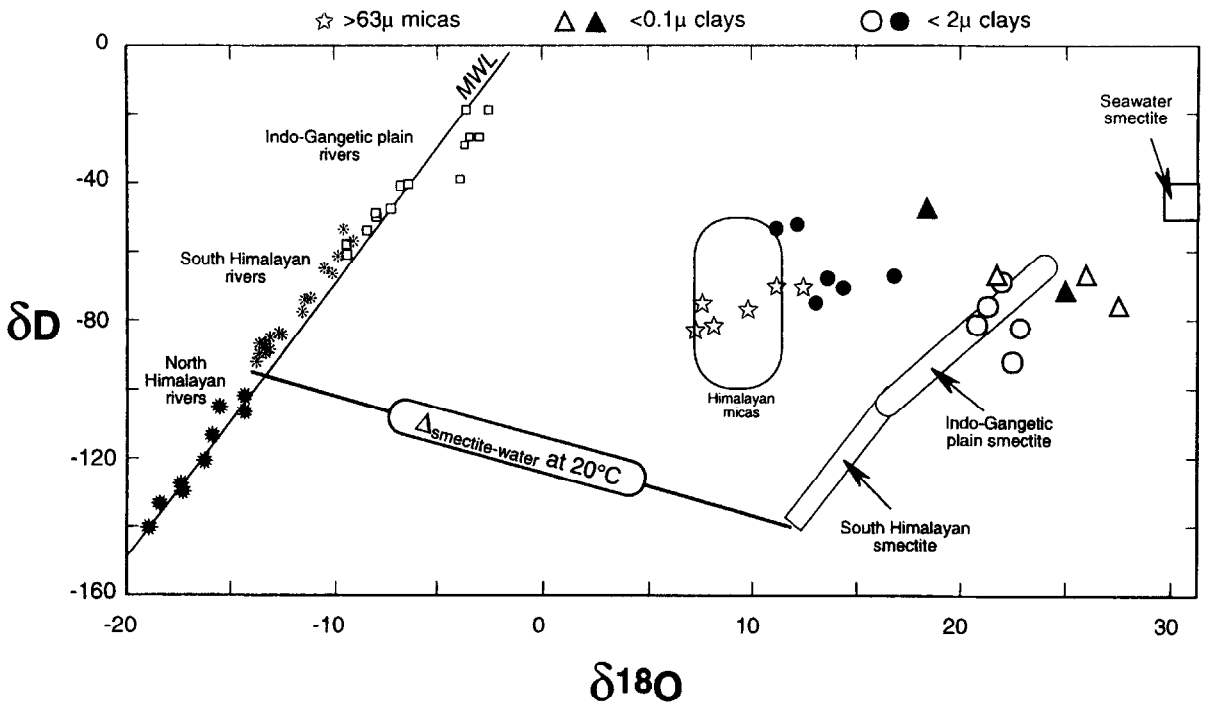

Fig. 5. $\delta^{18}O$ vs. δD for clays (Table 1) and micas [15] from the Bengal Fan. The central box is defined by measurements of HHC outcrop samples [25]. Fields for smectites in equilibrium with south flank Himalayan or Indo–Gangetic meteoric waters ([26] and unpublished data from the CRPG Nancy) are calculated using $\Delta^{H}_{sm-water}$ from [49] and $\Delta^{O}_{sm-water}$ from [28]. Smectite-rich samples are close to the isotopic equilibrium with meteoric waters of the Indo–Gangetic plain, fixing the location of the weathering environment.

for smectite–water [28] remains poorly defined at temperatures below 100°C, and uncertainties of 3–4‰ remain. For instance, the effect of chemical composition on smectite–water fractionation remains uncertain; smectite–water fractionation determined at 20°C for trioctahedral smectites is 33.7 but is 26.3 for dioctahedral smectites [28,29].

Despite some small uncertainty for oxygen isotopes, both hydrogen and oxygen isotopic compositions of SK clays are clearly too high to be in equilibrium with Himalayan surface waters, and too low to be in equilibrium with seawater or porewater. The stable isotope data instead require that the SK clays were produced at low elevation in the paleo-Gangetic plain.

6. Sr in secondary minerals

Sr in clay minerals resides principally in interlayer sites or adsorbed on mineral surfaces [30]. After treatment with exchange solutions, clay samples analyzed for this study contain significant Sr only in the interlayer sites. Exchange of interlayer cations is thought to be essentially complete during neoformation of smectites, and alteration of biotite to vermiculite, although the mechanism of exchange may differ [30]. Consequently, the isotopic composition of Sr from the treated pedogenic clay mineral separates represents the source of cations available at the time the interlayer sites were occupied during recrystallization or neoformation of the clays. In contrast to Nd isotopes, the $^{87}Sr/^{86}Sr$ values of treated pedogenic clays record the isotopic composition of the water present during alteration, and not that of the parent material. If Sr in Bengal Fan secondary clays was not subsequently reset during diagenesis, $^{87}Sr/^{86}Sr$ ratios of the clays can provide a record of the isotopic composition of water in the Gangetic flood plain through time.

We measured $^{87}Sr/^{86}Sr$ ratios in two types of pedogenic minerals from the Bengal Fan (Table 1).

Table 1
H, O, Sr and Nd isotopic data on grain size fractions and vermiculite separates from ODP Leg 116 samples of the Bengal Fan

Sample	Depth (mbsf)	Age (Ma)	Type (< øμ)	δD (‰)	$\delta^{18}O$ (‰)	Rb (ppm)	Sr (ppm)	$^{87}Sr/^{86}Sr$ (±0.00002)	$^{87}Rb/^{86}Sr$	$\epsilon_{Nd}(0)$ (±0.2)	Sm (ppm)	Nd (ppm)	K_2O/Al_2O_3
Hole 717C													
2X-1 (80–81)	15.8	0.1	2		*13.5*	*231.7*	*90.7*	*0.73723*	*7.39*	*−15.9*			
6X-2 (27–28)	47.8	0.3	2		*13.2*	*267.5*	*78.6*	*0.73810*	*9.88*	*−14.0*	*5.2*	*26.6*	0.190
15X-2 (49–50)	114.5	0.8	2			*208.6*	*82.4*	*0.74048*	*7.32*	*−13.4*			0.158
19X-CC (5–6)	150.5	1.0	2		*15.0*		*87.3*	*0.74006*		*−14.5*			0.160
20X-1 (76–77)	151.3	1.0	2	−67.3	16.9			*0.73791*					0.174
			Ver			404.3	51.3	0.71572	22.1	−14.8	2.5	11.5	
21X-4 (34–35)	164.8	1.1	2		22.1			*0.76224*		−20.5			0.099
28X-6 (19–20)	234.2	2.3	0.1	−67.0	21.9	137.0	44.0	0.72007		−12.3	9.4	40.3	0.107
			2			*209.5*	*40.4*	*0.72798*	*15.1*				0.173
29X-3 (110–111)	240.1	2.4	0.1	−67.0	26.1	52.9	10.0	0.73770		−16.9			0.067
			2	−65.1	22.8	*112.0*	*23.8*	*0.75484*	*13.7*	*−17.9*			0.097
30X-1 (116–117)	246.7	2.5	2	−92.6	22.6			*0.73851*					0.106
35X-6 (28–29)	301.4	3.4	2	−80.7	20.8			*0.74067*					0.094
40X-2 (90–91)	342.9	4.1	2	−75.5	*21.3*	*72.2*	*24.4*	*0.74220*	*8.58*				0.059
40X-6 (30–31)	348.3	4.2	2	−69.3	22.0	*64.0*	*25.0*	*0.75877*	7.34				0.071
41X-CC (33–34)	359.2	4.4	2		11.5		*72.8*	*0.75512*		−16.4			0.211
43X-5 (100–101)	376.0	4.7	2			*62.0*	*13.0*	*0.74476*					0.059
44X-2 (80–81)	380.8	4.8	2					*0.75891*		*−18.5*			
45X-7 (4–5)	397.0	5.0	2		19.6	*55.5*	*15.1*	*0.74836*	*10.7*				
50X-1 (141–142)	436.9	5.7	2					0.75158		−14.8			0.074
51X-4 (120–121)	450.7	5.9	2		23.2	54.0		*0.74058*		−11.7			0.062
54X-1 (59–60)	474.1	6.3	2			*56.0*	*29.0*	*0.73540*	*5.67*				0.069
54X-CC (25–26)	482.5	6.5	0.1	−75.9	27.7	40.9	26.0	0.72785		−13.8			0.026
55X-CC (45–46)	492.1	6.7	2		*21.1*	*75.1*	*25.7*	*0.73665*	*8.45*	−15.4			0.064
63X-1 (104–105)	560.0	7.6	2	−75.2	13.2	*301.0*	*17.0*	*0.75284*		*−14.4*		31.5	0.214
65X-3 (29–30)	581.3	7.9	2	−60.5	20.5					−17.2			0.074
75X-4 (25–26)	679.3	8.9	2	−61.4		*234.0*	*56.0*	*0.73628*	*12.0*	*−13.9*	5.1	26.3	0.188
77X-5 (132–133)	699.3	9.0	0.1	−71.5	25.1	46.4	9.2	0.71989		−11.9			0.034
85X-2 (83–84)	770.3	9.3	Ver			290.5	36.8	0.72101	22.1	−13.0	1.9	8.4	
Hole 718C													
57X-5 (70–71)	548.0	11.6	2	−68.0	13.7	*234.3*	*64.0*	*0.74003*	*10.6*				0.194
61X-1 (52–53)	579.8	12.0	0.1	−48.0	18.5		54.0	0.71274		−12.4		20.0	0.143
			2	−70.6	14.5								0.205
80X-1 (36–37)	761.7	14.3	2		15.8	279.1	65.3	0.73849	12.0	−14.4	8.0	38.5	0.208
			50			*104.4*	*59.9*	*0.75668*	*4.91*	*−16.7*	*3.7*	*19.8*	0.256
86X-2 (102–103)	820.8	15.1	Ver			262.4	58.1	0.72082	12.7	−14.7	3.3	13.7	
87X-2 (30–31)	829.6	15.2	2	−53.9	11.3	289.4	62.3	0.75265	13.1	−14.7	6.2	32.3	0.226
			50			*83.5*	*55.9*	*0.75494*	*4.21*	*−16.0*	*3.9*	*21.0*	0.274
88X-4 (30–31)	842.1	15.3	2			222.5	63.1	0.73603	9.92	−14.4	6.9	34.5	0.205
			50			*148.0*	*64.7*	*0.75767*	*6.44*	*−15.7*	*4.7*	*25.8*	0.266
89X-CC (13–14)	854.7	15.5	2			236.8	68.0	0.74161	9.80	−14.3	7.4	37.5	0.221
			50			*91.2*	65.1	*0.75307*	*3.94*	*−16.4*	*5.9*	*32.3*	0.254
90X-2 (44–45)	858.2	15.6	2			216.9	80.4	0.73683	7.58	−14.9	8.7	46.1	0.225
			50			*104.5*	*64.7*	*0.75085*	*4.55*	*−16.8*	*5.3*	*29.4*	0.271
			Ver			144.8	25.6	0.72336	15.9	−16.6	1.3	5.7	
96X-1 (31–32)	908.3	16.2	Ver			168.3	25.5	0.72049	18.6	−14.8	0.9	3.5	
97X-CC (10–11)	925.4	16.4	2	−52.8	12.3	233.5	61.8	0.74060	10.6	−14.5	6.7	35.9	0.225
			50			*110.6*	*64.5*	*0.75175*	*4.83*	*−16.0*	*3.8*	*20.4*	0.277
			Ver			124.5	50.0	0.72016	6.99	−15.0	0.6	2.4	

The first are < 2 μm and < 0.1 μm size fractions containing mostly smectite with lesser kaolinite. The second are separates of hand-picked vermiculite grains. There is significant variation in $^{87}Sr/^{86}Sr$ ratios of secondary clay mineral separates with age in the Bengal Fan (Fig. 5c). Samples older than 7.4 Ma are vermiculites and < 0.1 μm fractions, and have $^{87}Sr/^{86}Sr$ from 0.713–0.720 when corrected to age of deposition for Rb decay. Samples from 7.4 to 0.9 Ma are smectite-rich, and have $^{87}Sr/^{86}Sr$ from 0.73 to 0.76. A vermiculite sample younger than 0.9 Ma has $^{87}Sr/^{86}Sr$ of 0.715. High $^{87}Sr/^{86}Sr$ values in pedogenic clays are found during the interval of most intense weathering, as indicated by clay mineralogy and chemistry.

Diagenetic exchange with Sr in sediment pore water could affect the Sr isotope systematics of the secondary minerals. Data for pore waters from ODP Leg 116 show $^{87}Sr/^{86}Sr$ values increasing from seawater values near the sediment–water interface to a maximum of ca. 0.714 with depth (A. Michard, pers. commun.). The pattern of Sr isotopic variations in the pedogenic minerals from ODP 116 does not resemble the pore water profile. Fine-grained clay separates might be expected to exchange Sr with the pore waters faster than the much larger vermiculites, but most < 2 μm and < 0.1 μm samples are more radiogenic than either younger or older vermiculites. Although we cannot rule out some diagenetic exchange of Sr, we observe no systematic effect that can be attributed to this process. The pedogenic clays appear to retain their $^{87}Sr/^{86}Sr$ values established during neoformation or alteration. If 7–1 Ma smectites have undergone diagenetic exchange with pore water Sr, this would imply that their original values were even higher than the measured values.

Since in the GB plain, the $^{87}Sr/^{86}Sr$ of ground water do not differ significantly from that of nearby river water [31], the values of $^{87}Sr/^{86}Sr$ in pedogenic minerals suggest that the Sr isotopic composition of river water in the GB plain has varied widely since the early Miocene. Before ca. 7 and after 1 Ma $(^{87}Sr/^{86}Sr)_{RW}$ values were apparently similar to modern values for the major outflow of the GB rivers (0.719–0.725, [7]). However, from 7 to 1 Ma pedogenic clays record a major increase in the isotopic composition of dissolved Sr in the paleo-Gangetic plain. Estimated $(^{87}Sr/^{86}Sr)_{RW}$ values range from 0.74 to 0.76 in the early to middle Pliocene. Our interpretation of the Sr isotope data from the pedogenic minerals as a record of variation of $(^{87}Sr/^{86}Sr)_{RW}$ in the Himalayan foreland is in agreement with [32], who found a similar pattern of Sr isotopic variations in paleosol and fresh water shell carbonates from the Miocene–Pliocene Siwalik foreland basin sequence of Nepal. Given that these two sets of measurements are entirely independent, we believe that the evidence for high $(^{87}Sr/^{86}Sr)_{RW}$ in paleo-Gangetic flood plain waters during the Pliocene is strong.

7. Weathering processes and riverine $^{87}Sr/^{86}Sr$ history

As a first approximation, we can consider Sr in the GB system to have three sources. The first is carbonate weathering, which is likely to have $^{87}Sr/^{86}Sr \geq 0.710$, because carbonates in the GB drainage come from both unaltered rocks in India and the Tethyan Himalaya (≤ 0.709), as well as marbles in the HHC and TSS (≈ 0.710–0.714, [33]) and in the LH (≈ 0.8, but low [Sr], France-Lanord unpublished data). The fraction of carbonate Sr in the modern Ganges has been estimated to be ca. 70% [7], but the end members for this mixing calculation are not well constrained. The second is weathering of feldspars and other less resistant phases from the

Ages calculated from [47] recalibrated after [48]. Ver = > 63 μm vermiculite separates. Data in italics are from [11,17]. O and H isotope data relative to VSMOW. $^{87}Sr/^{86}Sr$ and $^{143}Nd/^{144}Nd$ measured on a Finnigan 262 (CRPG) or VG-54 (Cornell) thermal ionization mass spectrometer. $^{87}Sr/^{86}Sr$ values are corrected for fractionation with $^{86}Sr/^{88}Sr = 0.1194$ and normalized NBS-987 = 0.710230, $^{143}Nd/^{144}Nd$ values are corrected for fractionation with $^{146}Nd/^{144}Nd = 0.7219$ and normalized to La Jolla Nd = 0.511853. $\epsilon_{Nd}(0) = (^{143}Nd/^{144}Nd/CHUR\text{-}1)10^4$, where CHUR = 0.512638. Rb, Sr, Sm and Nd analyses were by isotope dilution. K_2O/Al_2O_3 measured by atomic absorption.

HHC ($^{87}Sr/^{86}Sr \approx 0.74$). The third is radiogenic Sr (≥ 0.8) derived from either the LH or high Rb/Sr micas from the HHC. Work in progress should provide better constraints on the isotopic compositions of current sources of dissolved Sr, which are needed to establish a robust Sr isotopic mass balance in the modern GB system, as well as for understanding past variations.

The high values of $(^{87}Sr/^{86}Sr)_{RW}$ recorded in Pliocene samples can result from changing sources of dissolved Sr, and/or changes in silicate mineral weathering intensity. The magnitude of the shift in $(^{87}Sr/^{86}Sr)_{RW}$ suggests that a decrease in the ratio of carbonate- to silicate-derived Sr weathering flux was at least partly responsible. A shift in the primary silicate source of dissolved Sr could also have changed the river isotopic ratio. Edmond [6] has argued that weathering of silicates from the HHC is currently the principal source of dissolved radiogenic Sr in the GB river system. If this is correct, an increased contribution from the radiogenic LH could result in higher $(^{87}Sr/^{86}Sr)_{RW}$. Nd isotopic data from the Bengal Fan record a few atypically low values during the Pliocene, which are consistent with a slightly increased contribution of LH material to the clastic load (Fig. 6c). Thus it is possible that a relative increase in Sr derived from the LH contributed to high $(^{87}Sr/^{86}Sr)_{RW}$ in the Pliocene, but the Nd data preclude a major change in silicate weathering provenance.

Weathering intensity of silicates can affect the $^{87}Sr/^{86}Sr$ of Sr released to solution during incongruent weathering [31,34–36]. As a simplification, we can consider the mineralogical composition of HHC rocks to consist of quartz, feldspar and micas (biotite and muscovite). Although crystallization/peak metamorphic ages for exposed Himalayan leucogranites and gneisses are near 20 Ma, biotites (and some muscovites) in the HHC can have $^{87}Rb/^{86}Sr$ ratios from 150 to 1000, and present day $^{87}Sr/^{86}Sr$ can be evolved to 0.8 or > 1 [17,33]. Under conditions of low weathering intensity, such as prior to 7 Ma or

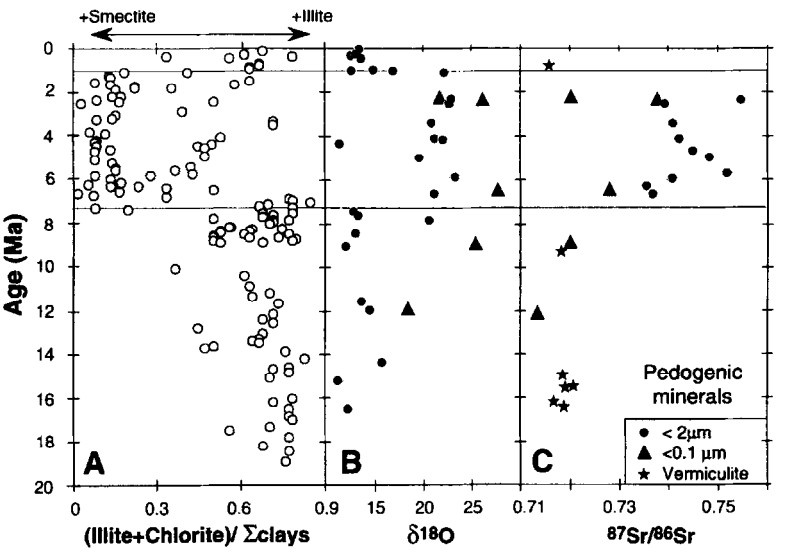

Fig. 6. (A) clay mineralogy from [15]. (Illite + chlorite)/Σclay ratios were obtained from XRD on < 2 μm fractions. They primarily reflect the relative abundance of illite vs. smectite. (B) $\delta^{18}O$ of < 2 μm fractions are correlated with clay mineralogy and chemistry (Table 1). Low $\delta^{18}O$ of illite- and chlorite-rich samples reflect the high-temperature provenance of these minerals, whereas smectite-rich samples have high $\delta^{18}O$, produced by low-temperature weathering reactions. (C) $^{87}Sr/^{86}Sr$ of secondary minerals as a function of age in the Bengal Fan. Secondary minerals are smectite-rich clay fractions (< 2 μm or < 0.1 μm) and coarse (ca. 200 μm) vermiculites. Tie lines connect < 0.1 μm and < 0.2 μm fractions from the same samples. The samples have been pre-treated to remove adsorbed Sr and other cations, and the Sr analyzed here is dominated by cations in the interlayer sites. The Sr in the interlayer sites records the $^{87}Sr/^{86}Sr$ of water present during recrystallization or neoformation of the secondary (pedogenic) clays. We interpret these data as a proxy record of the $^{87}Sr/^{86}Sr$ value of dissolved Sr in the Ganges–Brahmaputra river system (R_{GB}).

after 1 Ma in the Himalayan foreland, feldspar weathering ($^{87}Sr/^{86}Sr \approx 0.74$) is likely to dominate, while micas are only partly altered. During the Pliocene, flood plain weathering resulted in the production of abundant smectites indicating more intense weathering of micas. Weathering of HHC-derived micas in the Gangetic flood plain was very likely an important source of radiogenic Sr, despite lower Sr concentrations in micas than in feldspars. Additionally, the metamorphic rocks of the HHC contain abundant (near 30%) biotite and muscovite. Thus, a great deal of highly radiogenic micas are available for weathering in the GB system. We suggest that the increase in silicate weathering intensity recorded in Bengal Fan clay chemistry and mineralogy was an important driver for increased $(^{87}Sr/^{86}Sr)_{RW}$ during the late Miocene and Pliocene. This hypothesis makes specific predictions for the geochemistry of other elements, discussed below.

8. Comparison with the marine $^{87}Sr/^{86}Sr$ record

The flux of Sr from the Himalaya is often cited as an important force in quantitative models for the observed increase of marine $^{87}Sr/^{86}Sr$ in the late Cenozoic [1,4,5,7,10]. However, neither the flux nor its isotopic ratio have been well constrained. The evolution of the isotopic ratio of Sr in seawater can be given as:

$$\frac{dR_{SW}}{dt} = \frac{1}{\tau_{Sr}} \cdot \sum_i \frac{J_i}{J_{tot}} [R_i - R_{SW}] \qquad (1)$$

where the J_i and R_i are the fluxes and ratios of sources of Sr to the oceans, and τ_{Sr} is the oceanic residence time of Sr [35,37]. Following [5], we have calculated the rate of change of seawater $^{87}Sr/^{86}Sr$ using the record of $(^{87}Sr/^{86}Sr)_{RW}$ from the Ganges–Brahmaputra (R_{GB}) obtained here and assuming present day fluxes for all sources of Sr to the oceans, including the GB (Fig. 7b). The high Pliocene values of R_{GB} yield calculated rates of change (dR_{SW}/dt) that are up to an order of magnitude faster than the 'best fit' values observed over the last 7 Ma, and a factor of 3 greater than even the fastest short-term perturbations observed in this interval [38]. Two points are evident from this exercise: (1) changes in the $^{87}Sr/^{86}Sr$ of GB river water were capable of driving rapid shifts in the marine Sr isotopic budget; and (2) the flux of dissolved Sr from the GB system

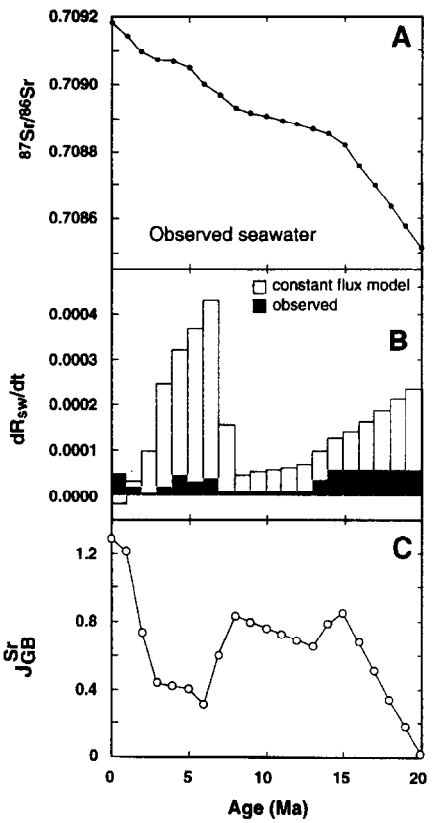

Fig. 7. (A) $^{87}Sr/^{86}Sr$ evolution curve for Neogene seawater [38,50]. (B) Rate of change of $^{87}Sr/^{86}Sr$ ratio of seawater with time (dR_{SW}/dt) calculated from the observed curve (A) and Eq. (1), assuming: (1) that the flux of Sr from the Ganges–Brahmaputra rivers (J_{GB}^{Sr}) is constant and equal to the modern flux; and (2) time-dependent $^{87}Sr/^{86}Sr$ (R_{GB}) according to Fig. 6c. The modeled rate of change exceeds the observed rate by up to an order of magnitude in the Pliocene, requiring a significant decrease in J_{GB}^{Sr} to fit the observed seawater curve. (C) Modeled flux of Sr from the GB rivers calculated to fit the observed $^{87}Sr/^{86}Sr$ evolution curve for seawater assuming variable R_{GB}, and holding all other sources of Sr to the oceans at present-day fluxes and ratios, as given in [5]. Values of flux calculation are normalized to a modern J_{GB}^{Sr} of 1.27×10^9 mol yr^{-1} [3]. The modern value calculated here exceeds the estimate of [3] by about 30%, which is the same result obtained by [5]. This discrepancy may result from the simplifications made here and in [5], or from an underestimate of the modern J_{GB}^{Sr} in [3], who did not sample during the main monsoon season. The low values of J_{GB}^{Sr} from 7 to 2 Ma correspond to the interval of intensified chemical weathering and low sedimentation rates recorded in the Bengal Fan.

must have been much lower in the Pliocene than at present.

The discrepancy between calculated and observed rates of seawater isotopic change in the early and middle Miocene has been discussed previously by Richter et al. [5] in terms of increasing Himalayan and Tibetan contributions to the riverine Sr flux with time. They assumed a constant value (modern) for $^{87}Sr/^{86}Sr$ in Himalayan and Tibetan rivers since 40 Ma, and estimated the change in Himalayan and Tibetan Sr flux necessary to satisfy the observed marine $^{87}Sr/^{86}Sr$ record, while holding all other fluxes and their isotopic ratios at modern values. We repeat this calculation over the last 20 Ma using our clay proxy records of GB isotopic composition, and solve Eq. (1) for the Sr flux from the GB system (J_{GB}^{Sr}) as a function of time (Fig. 7c). In this calculation, J_{GB}^{Sr} depends essentially on dR_{SW}/dt and R_{GB}. The data from secondary phases from 17 to 7 Ma imply that R_{GB} was approximately constant near 0.719, and consequently the J_{GB}^{Sr} curve through this interval is similar to that calculated by [5]. As they noted, a generally increasing Himalayan Sr flux is necessary to satisfy the marine Sr record during this interval, with a peak value near 16 Ma. However, the high R_{GB} values after 7 Ma requires a ca. 50% decrease in the flux of Sr from the Himalaya.

The interval of rapid change in $(^{87}Sr/^{86}Sr)_{SW}$ beginning near 6 Ma (Fig. 6a) could be explained by either an increase in the global Sr river flux, or by an increase in the global mean $^{87}Sr/^{86}Sr$ of rivers. The proxy record of GB isotopic composition strongly supports the latter scenario, with even larger changes in river $^{87}Sr/^{86}Sr$ than those proposed by [4]. The decrease in GB Sr flux after 7 Ma required by the proxy data differs from the history suggested by [5], but is similar to that suggested from studies that use the combined records of Nd and Sr isotopic variations in sea water [1,10]. These models find a decrease in global river Sr flux in the Mio–Pliocene, which is consistent with our results, suggesting that coupling of the isotopic records of Nd and Sr can be an effective means to constrain past variability in riverine Sr isotopic ratios.

The calculated GB Sr flux rises dramatically in the Pleistocene, driven both by a return to lower R_{GB} and an increase in observed dR_{SW}/dt. The increase in J_{GB}^{Sr} is correlated with a return to high sedimentation rates and low weathering intensity in the middle Pliocene. There is a generally inverse correlation between Sr concentration [Sr] in river waters and isotopic ratio, which reflects both congruent dissolution of carbonates and the slower kinetics of incongruent weathering of silicate minerals [6,9]. Although Himalayan rivers define a steeper trend for $1/[Sr]$ vs. $^{87}Sr/^{86}Sr$ than other world rivers, the form of this relation appears valid there as well [31]. The time evolution of Neogene Sr flux from the Himalaya described above consists of a late Miocene to mid-Pleistocene interval of high weathering intensity and low Sr flux, bracketed by intervals of low weathering intensity and high Sr flux. This evolution is thus consistent with the $[Sr]$–$^{87}Sr/^{86}Sr$ relations known from modern rivers.

9. Neogene erosion and weathering of the Himalaya

The Bengal Fan record of Sr input to the oceans shows that the $^{87}Sr/^{86}Sr$ ratio of dissolved Sr increased significantly near 7.4 Ma. Simultaneously, in order to accommodate the marine isotopic record of Sr, the Sr flux of the GB rivers must have decreased. The rise of $^{87}Sr/^{86}Sr$ ratios and decrease of Sr flux imply an increased contribution from silicate weathering relative to carbonate dissolution. Because of kinetic limitations on rates of silicate weathering these changes suggest that the residence time of sediments in the weathering environment increased near 7 Ma as well. An increase in sediment residence time in the flood plain–foreland basin is consistent with the sedimentological history of the Siwalik foreland basin and the Bengal Fan. The history of drainage patterns of the paleo-Ganges suggests a wide flood plain with sediment loading rather than thrust loading, primarily responsible for subsidence in the Pliocene [39]. After 7.4 Ma, sedimentation in the Bengal Fan shifts to fine-grained silts and muds and lower accumulation rates, implying that both transport energy and sediment flux decreased. Isotopic analysis of organic carbon deposited in the Fan after 7.4 Ma demonstrates a large flux from C4 plants which inhabited the paleo-Gangetic flood plain [8,22]. The abundances of C4 plant-derived carbon and smectite clay are highly correlated in Bengal Fan sediments, and suggest that floodplain weathering

took place in soils stabilized by C4 grasses. Silicate weathering rates and intensity could also have increased in response to a change toward a monsoonal climate, but this climatic shift alone would not result in the substantially decreased Sr flux necessary to fit the observations. If silicate weathering rates increased while the supply of fresh sediment remained constant, an increase in Sr flux would result, opposite to that calculated from the isotopic data above. Therefore, we interpret the decrease in Sr flux in the late Miocene to be the result of decreased erosion rates in the Himalaya. A decrease in erosion rate of the Himalaya starting ca. 7 Ma ago is in good agreement with independent sedimentological changes in the Bengal Fan (Fig. 2). Sedimentation and subsidence in the Siwalik foreland basin sequence do not show a compensating increase in accumulation in this interval, implying a general reduction in the clastic sediment flux from the Himalaya over the late Miocene to Pleistocene interval [40].

The change in the erosional regime near 7 Ma is accompanied by simultaneous ecological change in the basin [8,21,22]. During the same interval, paleoceanographic markers of upwelling in the Arabian Sea suggest an intensification of the Asian monsoon [41]. The synchroneity of these changes suggest that climate variation is a common control on both erosion and vegetation. Increased monsoon activity in the late Miocene appears to have resulted in increased weathering intensity but, perhaps counter-intuitively, decreased physical erosion and Sr flux. However, a reduction in erosion rate resulting from climate changes alone has implications for the elevation history of the Himalaya. After accounting for isostatic compensation, the mean elevation of the range is set by the balance between tectonic uplift and denudation rates [42]. A late Miocene decrease in erosional denudation would result in increased mean elevation of the range, unless it were accompanied by decreased rates of uplift. We find that the simplest way to resolve a long term increase in weathering intensity and decrease in sediment supply during the late Miocene–Pliocene is a reduction in the tectonic uplift rate of the Himalaya.

The marked increase in sediment accumulation and calculated Sr flux from the GB system in the middle Pleistocene is associated with a major change in the weathering environment and a return to low weathering intensity. We surmise that increased mid-Pleistocene glaciation in the Himalayan region contributed to the change in weathering environment and increased sediment flux. We suggest that a Pleistocene increase in the tectonic rate of uplift is also necessary to maintain the high mean elevation and steep relief of the present Himalaya in the face of enhanced Pleistocene erosion rates.

10. Implications for fluxes of other elements

Our estimate of Neogene Sr fluxes and weathering intensity variations in the GB river system has implications for the fluxes of some other elements. The decreased Sr flux beginning in the late Miocene implies a decreased flux of Ca ± Na, because these elements are highly correlated in most river waters [35,43]. The increase in weathering intensity in the GB system should affect silica fluxes as well. High Si/(Na + K) values (reflecting high silicate weathering intensity) are associated with low Sr concentrations in rivers draining the Guyana shield [31]. Weathering intensity is also positively correlated with Ge/Si ratios but negatively correlated with Si concentrations in many rivers [44]. The increase in silicate weathering intensity inferred for the GB beginning in the late Miocene should, therefore, be associated with a decrease in Si flux and an increase in Ge/Si ratio coming from the GB river system. The global marine Ge/Si ratio increases near 7 Ma [45], which could reflect Himalayan inputs. A further consequence of this change in weathering flux is probably decreased CO_2 consumption by silicate weathering.

A number of paleoceanographic records show important variations in the late Miocene to Pliocene. Records of $CaCO_3$ deposition (or CCD depth) show increases at a number of Indian and Pacific ocean sites [46]. Our inference of decreased Sr and Ca fluxes from the Himalaya during this time implies that changes in Himalayan weathering did not result in increased carbonate deposition by increasing the Ca^{2+} flux to the oceans. Either another source of Ca increased enough to more than offset the decrease in the Himalayan flux near this time, or the observed changes in carbonate MAR do not reflect increased

Ca fluxes to the oceans. In contrast, the observed positive shifts in marine Ge/Si and $^{87}Sr/^{86}Sr$ near 6–7 Ma are consistent with increased weathering intensity in the GB system.

11. Conclusion

The sedimentary record of the Bengal Fan documents past variations of the erosion and weathering regime in the Ganges–Brahmaputra basin which drains much of the Himalaya. The Leg 116 and DSDP 218 cores from the Bengal Fan record a clear change near 7.4 Ma, from an erosion regime dominated by physical erosion to one with significant chemical weathering — this change is reversed at ca. 1 Ma. Increased weathering intensity from the late Miocene to middle Pleistocene results in the production of smectite-rich sediments by weathering detritus from high grade metamorphic rocks. Oxygen and hydrogen isotope data show that the principal site of chemical weathering during this interval was the GB plain. The change in the weathering environment increases the isotopic composition of the riverine Sr in the GB system from ≈ 0.72 to > 0.74. This increase requires a significant decrease in the GB flux of Sr to the oceans in order to fit the observed evolution of the Pliocene marine $^{87}Sr/^{86}Sr$ record, unless there are quite large coeval changes in Sr fluxes from other sources. It is highly probable that fluxes of some other elements from the GB, including Ca, Na and Si, also decreased.

The Ganges–Brahmaputra example underlines the importance of the different processes involved during continental erosion. This study shows that changes in weathering intensity can have as large an impact on the marine Sr budget as can changes in uplift and erosion. Some may find it paradoxical to observe that, during the Mio–Pliocene, reduced erosion of the Himalaya and reduced Himalayan Sr flux result in increased $^{87}Sr/^{86}Sr$ of the oceans, and that these changes coincide with an interval of increased monsoon intensity. The variation in the relative importance of physically dominated erosion, which mainly dissolves Sr from carbonates, and chemical weathering, which releases Sr from radiogenic silicates, exert a primary long term control on the Himalayan input of Sr to the oceans.

While the general effect of continental erosion on the oceanic budget of Sr is clear, detailed study of a single orogeny shows that large variations in both flux and isotopic composition of Sr can occur within a geologically short time span. Interpretation of the marine Sr record in terms of variable erosional flux, global silicate weathering or mountain uplift based on the extrapolation of our knowledge of present fluxes or isotope ratios can be misleading because changes occurring at regional scale can significantly affect this record.

Acknowledgements

We especially thank Albert Galy for identification and Sr analyses of vermiculites. We are grateful to Annie Michard, Jay Quade, and Doug Burbank for discussions during this study, and we thank John Compton and Martin Palmer for careful reviews. This work was supported by the CNRS–INSU through the program DBT 'Fleuves et Erosion' (contribution 48). CRPG contribution 1201. *[FA,UC]*

References

[1] S.B. Jacobsen, Isotopic constraints on crustal growth and recycling, Earth Planet. Sci. Lett. 90, 315–329, 1988.

[2] M.E. Raymo, W.F. Ruddiman and P.N. Froelich, Influence of late Cenozoic mountain building on ocean geochemical cycles, Geology 16, 649–653, 1988.

[3] M.R. Palmer and J.M. Edmond, The strontium isotope budget of the modern ocean, Earth Planet. Sci. Lett. 92, 11–26, 1989.

[4] D.A. Hodell, G.A. Mead and P.A. Mueller, Variation in the strontium isotopic composition of seawater (8 Ma to present): Implications for chemical weathering rates and dissolved fluxes to the oceans, Chem. Geol. 80, 291–307, 1990.

[5] F.M. Richter, D.B. Rowley and D.J. DePaolo, Sr isotope evolution of seawater: the role of tectonics, Earth Planet. Sci. Lett. 109, 11–23, 1992.

[6] J.M. Edmond, Himalayan tectonics, weathering processes, and the strontium isotope record in marine limestones, Science 258, 1594–1597, 1992.

[7] S. Krishnaswami, J.R. Trivedi, M.M. Sarin, R. Ramesh and K.K. Sharma, Strontium isotopes and rubidium in the Ganga–Brahmaputra river system: Weathering in the Himalaya, fluxes to the Bay of Bengal and contributions to the evolution of oceanic $^{87}Sr/^{86}Sr$, Earth Planet. Sci. Lett. 109, 243–253, 1992.

[8] C. France-Lanord and L.A. Derry, $\delta^{13}C$ of organic carbon in

the Bengal fan: source evolution and transport of C3 and C4 plant carbon to marine sediments, Geochim. Cosmochim. Acta 58, 4809–4814, 1994.

[9] F. Albarède and A. Michard, Evidence for slowly changing $^{87}Sr/^{86}Sr$ in runoff from fresh water limestones of southern France, Chem. Geol. 64, 55–65, 1988.

[10] A.J. Kaufman, S.B. Jacobsen and A.H. Knoll, The Vendian record of Sr- and C-isotopic variations in seawater: Implications for tectonics and paleoclimate, Earth Planet. Sci. Lett. 120, 409–430, 1993.

[11] C. France-Lanord, L. Derry and A. Michard, Evolution of the Himalaya since Miocene time: isotopic and sedimentologic evidence from the Bengal Fan, in: Himalayan Tectonics, P.J. Treloar and M. Searle, eds., Geol. Soc. London Spec. Publ. 74, 603–621, 1993.

[12] J.R. Curray, Sediment volume and mass beneath the Bay of Bengal, Earth Planet. Sci. Lett. 125, 371–383, 1994.

[13] J.R. Cochran, Himalayan uplift, sea level, and the record of Bengal fan sedimentation at the ODP Leg 116 Sites, in: Proc. ODP Sci. Results 116, 397–414, 1990.

[14] Shipboard Scientific Party, Initial Reports Sites 717-718-719 Distal Bengal Fan, Proc. ODP Init. Rep. 116, 1989.

[15] A. Bouquillon, C. France-Lanord, A. Michard and J.-J. Tiercelin, Sedimentology and isotopic chemistry of the Bengal fan sediments: the denudation of the Himalaya, Proc. ODP Sci. Results, 116, 43–58, 1990.

[16] D.A.V. Stow, K. Amano, P.S. Balson, G.W. Brass, J. Corrigan, C.V. Raman, J.-J. Tiercelin, M. Townsend and N.P. Wijayananda, Sediment facies and processes on the distal Bengal Fan, Leg 116, Proc. ODP Sci. Results 116, 377–396, 1990.

[17] A. Galy, C. France-Lanord and L.A. Derry, Oligo–Miocene uplift and unroofing of the Himalaya: evidence from the Bengal Fan, Tectonophysics, in press.

[18] A. Bouquillon, H. Chamley and F. Fröhlich, Sédimentation argileuse au Cénozoïque supérieur dans l'océan Indien Nord-oriental, Ocean. Acta 12, 133–147, 1989.

[19] S. Gartner, D.A. Johnson and B. McGrowran, Paleontology synthesis of deep sea drilling results from Leg 22 in the Northeastern Indian Ocean, Init. Rep. DSDP 22, 805–813, 1974.

[20] Shipboard Scientific Party, Site 222, Init. Rep. DSDP 23, 211–289, 1974.

[21] J. Quade, T.E. Cerling and J.R. Bowman, Development of Asian monsoon revealed by marked ecological shift during the latest Miocene in northern Pakistan, Nature 342, 163–166, 1989.

[22] J. Quade, J.M.L. Cater, T.P. Ojha, J. Adam and T.M. Harrison, Late Miocene environmental change in Nepal and the northern Indian subcontinent: stable isotopic evidence from paleosols, Geol. Soc. Am. Bull. 107(12), 1381–1397, 1995.

[23] A.C. Pimm, Mineralization and trace element variation in deep-sea pelagic sediments of the Wharton basin, Indian Ocean, Init. Rep. DSDP 22, 469–476, 1974.

[24] P.L. Manley and R.D. Flood, Cyclic sediment deposition within the Amazon deep-sea fan, AAPG Bull. 72, 912–925, 1988.

[25] C. France-Lanord, S.M.F. Sheppard and P. Le Fort, Hydrogen and oxygen isotope variations in the High Himalaya peraluminous Manaslu leucogranite: evidence for heterogeneous sedimentary sources, Geochim. Cosmochim. Acta 52, 513–526, 1988.

[26] R. Ramesh and M.M. Sarin, Stable isotope study of the Ganga (Ganges) river system, J. Hydrol. 139, 49–62, 1992.

[27] J. Boulègue and T. Bariac, Oxygen and hydrogen isotope ratios of interstitial waters from an intraplate deformation area: Bengal Fan, Leg 116, Proc. ODP Sci. Results, 116, 127–133, 1990.

[28] H.W. Yeh and S.M. Savin, Mechanism of burial metamorphism of argillaceous sediments: 3. O-isotope evidence, Geol. Soc. Am. Bull. 88, 1321–1330, 1977.

[29] M.A. Escande, Echangeabilité et fractionnement isotopique de l'oxygène des smectites magnésiennes de synthèse. Etablissement d'un géothermomètre, Thèse de 3ème cycle, Orsay, 1983.

[30] M.B. McBride, Environmental Chemistry of Soils, Oxford Univ. Press, Oxford, 1994.

[31] M.R. Palmer and J.M. Edmond, Controls over the strontium isotope composition of river water, Geochim. Cosmochim. Acta 56, 2099–2111, 1992.

[32] J. Quade, Major shifts in the $^{87}Sr/^{86}Sr$ ratios of large paleorivers draining the Himalayas of central Nepal over the past 10 Ma, Geol. Soc. Am. Abstr. Progs. 25(6), 175, 1993.

[33] C. Deniel, Apport des isotopes du Sr, du Nd et du Pb à la connaissance de l'âge et de l'origine des leucogranites himalayens. Exemple du Manaslu (Himalaya, Népal), Univ. Clermont-Ferrand, 1985.

[34] E.J. Dasch, Strontium isotopes in weathering profiles, deep sea sediments and sedimentary rocks, Geochim. Cosmochim. Acta 33, 1521–1552, 1969.

[35] S.J. Goldstein and S.B. Jacobsen, The Nd and Sr isotopic systematics of river-water dissolved material: implications for the sources of Nd and Sr in seawater, Chem. Geol. 66, 245–272, 1987.

[36] J.D. Blum and Y. Erel, A silicate weathering mechanism linking increase in marine $^{87}Sr/^{86}Sr$ with global glaciation, Nature 373, 415–418, 1995.

[37] G.W. Brass, The variation of the marine $^{87}Sr/^{86}Sr$ ratio during Phanerozoic time: interpretation using a flux model, Geochim. Cosmochim. Acta 40, 721–730, 1976.

[38] J.W. Farrell, S.C. Clemens and L.P. Gromet, Improved chronostratigraphic reference curve of late Neogene seawater $^{87}Sr/^{86}Sr$, Geology 23, 403–406, 1995.

[39] D.W. Burbank, Causes of recent Himalayan uplift deduced from deposited patterns in the Ganges basin, Nature 357, 680–683, 1992.

[40] D.W. Burbank, L.A. Derry and C. France-Lanord, Reduced Himalayan sediment production 8 Myr ago despite an intensified monsoon, Nature 364, 48–50, 1993.

[41] W.L. Prell, D.W. Murray and S.C. Clemens, Evolution and variability of the Indian Ocean Summer Monsoon: Evidence from the Western Arabian Sea Drilling Program, in: Synthesis of Results from Scientific Drilling in the Indian Ocean, R.A. Duncan, D.K. Rea, R.B. Kidd, U. von Rad and J.K.

Weissel, eds., Am. Geophys. Union Geophys. Monogr. 70, 447–469, 1992.

[42] P. Molnar and P. England, Late Cenozoic uplift of mountain ranges and global climate change: chicken or egg?, Nature 346, 29–34, 1990.

[43] P.S. Andersson, G.J. Wasserburg, J. Ingri and M.C. Stordal, Strontium, dissolved and particulate loads in fresh and brackish waters: the Baltic Sea and Mississippi Delta, Earth Planet. Sci. Lett. 124, 195–210, 1994.

[44] P.N.V. Froelich, R.A. Blanc, R.A. Mortlock, S.N. Chillrud, W. Dunstan, A. Udomkit and T.-H. Peng, river fluxes of dissolved silica to the ocean were higher during glacials: Ge/Si in diatoms, rivers, and oceans, Paleoceanography 7, 739–767, 1992.

[45] A. Shemesh, R.A. Mortlock and P.N. Froelich, Late Cenozoic Ge/Si record of marine biogeinc opal: Implications for variations in river fluxes to the ocean, Paleoceanography 4, 221–234, 1989.

[46] L.C. Petersen, D.W. Murray, W.U. Ehrmann and P. Hempel, Cenozoic carbonate accumulation and compensation depth changes in the Indian Ocean, in: Synthesis of Results from Scientific Drilling in the Indian Ocean, R.A. Duncan, D.K. Rea, R.B. Kidd, U. von Rad and J.K. Weissel, eds., Am. Geophys. Union Geophys. Monogr. 70, 311–333, 1992.

[47] S. Gartner, Neogene calcareous nannofossil biostratigraphy, Leg 116 (Central Indian Ocean), Proc. ODP Sci. Results 116, 165–187, 1990.

[48] S.C. Cande and D. Kent, A new geomagnetic polarity time scale for the late Cretaceous and Cenozoic, J. Geophys. Res. 97(B10), 13917–13951, 1992.

[49] S.M.F. Sheppard and A.H. Gilg, Stable isotope geochemistry of clay minerals, Clay Miner. 31, 1–24, 1996.

[50] J.S. Oslick, K.G. Miller, M.D. Feigenson and J.D. Wright, Oligocene–Miocene strontium isotopes: Stratigraphic revisions and correlations to an inferred glacioeustatic record, Paleoceanography 9, 427–443, 1994.